

1 **RADIATION DOSE AND ANTIOXIDANT DEPLETION IN A HDPE GEOMEMBRANE**

2
3 Kuo Tian¹, Craig H. Benson², Youming Yang³, and James M. Tinjum⁴

4
5 **ABSTRACT:** The impact of α and β radiation on antioxidant depletion in smooth high-density
6 polyethylene (HDPE) geomembranes (GMs) is described. Smooth HDPE GMs having different
7 thickness (0.04-mm, 0.1-mm, 0.2-mm) were created by mechanically pulverizing sections of 2-
8 mm-thick smooth HDPE GM and extruding the polymer at different thicknesses using a film
9 blowing machine. The 2-mm-thick smooth HDPE GM was also used in the experiments. HDPE
10 GM specimens were exposed to sealed sources of ²⁴¹Am and ⁹⁹Tc for 1–50 h to simulate the
11 impact of α and β radiation from U and ⁹⁹Tc in low-level radioactive waste (LLW) leachate.
12 Standard oxidative induction time (OIT) tests were conducted to determine antioxidant depletion.
13 No change in OIT occurred in the 2-mm-thick HDPE GM after exposure to sealed sources of
14 ²⁴¹Am and ⁹⁹Tc for 50 h. In much thinner GMs (e.g., 0.04 mm), however, significant antioxidant
15 depletion occurred after exposure most likely due to penetration of α and β particles. Penetration
16 depth of α and β particles and dose deposition in HDPE GMs were estimated with the GEometry
17 ANd Tracking (GEANT4) program. Predictions from GEANT4 show that maximum dose
18 deposition occurs at the surface of the HDPE GM and decreases with depth. A multilayer model
19 is used to estimate antioxidant depletion in HDPE GMs for depth-dependent doses. These
20 estimates suggest that radiation from LLW leachate has an insignificant effect on antioxidant
21 depletion in HDPE GMs due to the low dose deposition (e.g., 2.42 Gy) expected over a 1000-yr
22 service life, even if the level of activity in LLW leachate increases 10x to 100x the level typical of
23 today.

24

¹Assistant Professor, Sid and Reva Dewberry Department of Civil and Environmental Engineering, George Mason University, Fairfax, VA, USA, 22030, ktian@gmu.edu

²Dean, School of Engineering, University of Virginia, Charlottesville, VA, USA, 22904, chbenson@virginia.edu

³Assistant Professor, Department of Radiation Oncology, University of California, Los Angeles, CA, USA, 90095, youmingyang@mednet.ucla.edu

⁴Associate Professor, Department of Engineering Professional Development, University of Wisconsin-Madison, Madison, WI, USA, 53706, jmtinjum@wisc.edu

25 **Keywords:** HDPE Geomembrane, antioxidant depletion, low-level radioactive waste, radiation,
26 dose deposition, service life.
27

28 INTRODUCTION

29 Composite liners consisting of a geomembrane (GM) overlying a geosynthetic clay liner
30 or a compacted clay liner are used in low-level radioactive waste (LLW) and mixed waste (MW)
31 disposal facilities to limit release of contaminants (Powell et al. 2011, Tian et al. 2016, 2017a).
32 High-density polyethylene (HDPE) GMs are most common in LLW and MW facilities, consisting
33 of polymer resin (>95%), carbon black (2–3%), and antioxidant (0.5–1%) (Hsuan et al. 1998). The
34 longevity of HDPE GMs installed in LLW disposal facilities has particular importance in the US
35 because LLW and MW disposal facilities are required to have a service life in excess of 1000 yr
36 (DOE 2001). Conducting a performance assessment (PA) requires a method to estimate the rate
37 of degradation of HDPE GMs and their service life in LLW and MW facilities. Without a method to
38 estimate life expectancy, most PAs for LLW and MW facilities in the US ignore the contribution of
39 GMs to control flux from a disposal facility (Tian et al. 2017a).

40 Estimating life expectancy requires understanding the non-physical degradation of HDPE
41 GMs in their environment. HDPE GMs undergo non-physical degradation in three stages:
42 antioxidant depletion (Stage I), induction time to the onset of polymer degradation (Stage II), and
43 polymer property degradation (Stage III) (Grassie and Scott 1985, Hsuan and Koerner 1998,
44 Rowe and Sangam 2002, Gulec et al. 2004, Rowe et al. 2009, 2013, Tian et al. 2014, 2015,
45 2017a). The duration of Stage I (antioxidant depletion) is controlled by the rate of depletion of
46 antioxidants (Hsuan and Koerner 1998, Sangam and Rowe 2002, Rowe and Rimal 2008, Rowe
47 et al. 2008, 2009, 2010, 2013, Tian et al. 2014, 2017a).

48 Previous studies have demonstrated that leachate composition affects the rate of
49 antioxidant depletion in HDPE GMs (Osawa and Ishizuka 1973, Rowe and Sangam 2002, Gulec
50 et al. 2004, Rowe et al. 2009, 2013, Tian et al. 2014, 2017a). Gulec et al. (2004) report that metals

51 in acidic mine drainage (AMD) act as catalysts that accelerate decomposition of hydroperoxides,
52 resulting in generation of free radicals that consume antioxidants. Rowe et al. (2008) indicate that
53 surfactants in municipal solid waste (MSW) leachate accelerate the diffusive loss of antioxidants
54 by increasing partitioning between the GM and surrounding leachate. Tian et al. (2017a) indicate
55 that LLW leachates can promote radiative oxidation that consumes antioxidant if the dose is
56 sufficient.

57 LLW leachate consists of inorganic macrocomponents (e.g. Ca, Mg, Cl, SO_4^{2-}), trace
58 heavy metals (e.g., Fe, Cu), radionuclides (e.g., uranium, ^{226}Ra , and ^{99}Tc), and organic
59 compounds (Tian 2012, Tian et al. 2014, 2017a, b, Abdelaal and Rowe 2015). Tian et al. (2017b)
60 characterized the composition of LLW leachate based on field data collected from four LLW
61 disposal facilities operated by the US Department of Energy for environmental restoration
62 activities. U (6.4–3060 $\mu\text{g/L}$), ^{99}Tc (0.3–28 Bq/L), and ^3H (0.6–4629 Bq/L) were reported as the
63 primary radionuclides in the leachates having concentration above the detection limit (Tian et al.
64 2017b). Abdelaal and Rowe (2015) report that leachates in six LLW disposal facilities in Canada
65 contained ^{226}Ra (3.9–50 Bq/L) and ^{238}U (6–1500 $\mu\text{g/L}$). These radionuclides emit α (e.g., U and
66 ^{226}Ra) and β (^{99}Tc and ^3H) particles, which can cause radiation-induced oxidation in HDPE GMs
67 and accelerate degradation (Phillips 1988, Costa et al. 2008, Tian et al. 2017a).

68 Tian et al. (2017a) conducted accelerated aging experiments to predict antioxidant
69 depletion in a 2-mm-thick HDPE GM exposed to LLW leachate. A radioactive synthetic leachate
70 (RSL) was created to represent leachates at disposal facilities operated by the US Department of
71 Energy (Tian et al. 2017b). Comparative tests with non-radioactive synthetic leachate (NSL),
72 which is chemically the same as RSL but devoid of radionuclides, showed only 7% difference in
73 antioxidant depletion rates, suggesting that the effect of radiation from LLW leachate is limited.

74 The objective of this study was to estimate antioxidant depletion associated with the dose
75 that would be deposited on a HDPE GM over a 1000 yr period in response to radiation emitted

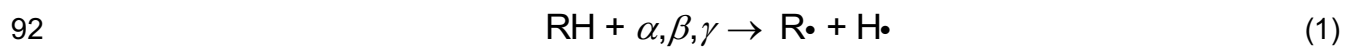
76 by radionuclides in typical LLW leachates, as well as leachates with higher radioactivity. Various
77 total doses and dose rates were applied to HDPE GM specimens by irradiation with sealed
78 sources of ^{99}Tc and ^{241}Am , which emit α and β particles that are present in LLW leachate and
79 could penetrate a HDPE GM in a LLW facility. Antioxidant depletion after irradiation was evaluated
80 by measuring the oxidation induction time (OIT) in HDPE specimens after exposure using
81 differential scanning calorimetry (DSC). Radionuclide decay and dose deposition in the HDPE
82 specimens were **estimated** using the GEometry ANd Tracking (GEANT4) program. Antioxidant
83 depletion data and predictions from the GEANT4 simulation were used as inputs to a multilayer
84 analytical model created to **estimate** antioxidant depletion as a function of dose deposition for
85 different scenarios.

86

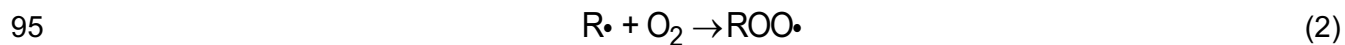
87 **BACKGROUND**

88 **Effect of Radiation on Degradation of HDPE GM**

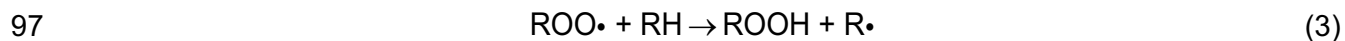
89 Polymer chains (RH) can dissociate into a free radical polymer chain ($\text{R}\bullet$) and hydrogen
90 ($\text{H}\bullet$) when exposed to ionizing radiation having energy exceeding the energy associated with the
91 covalent bond in the polymer chain (Phillips 1998, Peacock 2000):



93 where α , β , and γ are sources of ionizing radiation. The $\text{R}\bullet$ generated by ionizing radiation can
94 react with oxygen (O_2) to form $\text{ROO}\bullet$:



96 and $\text{ROO}\bullet$ can react with RH to form ROOH and more $\text{R}\bullet$ (Eq. 3):



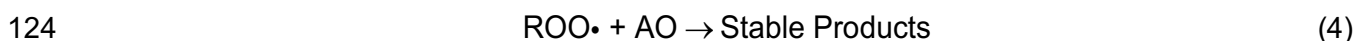
98 This sequence of reactions is defined as radiation-induced oxidation (Mason et al. 1993, Peacock
99 2000, Costa et al. 2008, Tian et al. 2017b).

100 Polymer degradation is affected by the type and energy of radiation (Phillips 1988,
101 Czikovszky 2004, Turner 2007). Charged α particles penetrate polymers on the order of microns,
102 charged β particles on the order of millimeters, and uncharged particles (e.g., neutrons and γ
103 rays) can penetrate meters (Turner 2007). Therefore, α and β particles typically affect the surface
104 of a GM, whereas γ rays can affect the entire thickness of a GM (Tian et al. 2017a). A penetrating
105 particle causes damage when the ionizing radiation associated with the particle has sufficient
106 energy to exceed the carbon-carbon bond energy. The α particles emitted from U (e.g., peak
107 energy from $^{238}\text{U} = 4.27$ MeV) and ^{226}Ra (e.g., peak energy = 4.87 MeV) and β particles from ^{99}Tc
108 (e.g., peak energy: 294 keV) are the predominant sources of radiation from LLW (Abdelaal and
109 Rowe 2015, Tian et al. 2017b). Ionizing radiation associated with α and β particles has sufficient
110 energy to exceed the typical bond energy of carbon-carbon bonds in polymers (5–10 eV,
111 Czikovszky 2004). Thus, α and β particles from LLW leachate can break bonds in HDPE GMs,
112 and promote antioxidant depletion.

113

114 **Effect of Radiation on Antioxidant Depletion**

115 Mason et al. (1993) examined the effect of γ radiation on antioxidant depletion in ethylene
116 propylene rubber (EPR) and cross-linked polyethylene (XLPE) cable insulation used in nuclear
117 power plants. The EPR and XLPE were prepared with different antioxidant packages and
118 concentrations. Antioxidant depletion was monitored using standard oxidative induction time
119 (OIT) tests according to ASTM D3895. Mason et al. (1993) report that OIT is exponentially related
120 to antioxidant concentration initially added to the polymer and decreases exponentially as a
121 function of exposure time at a constant irradiation dose. Mason et al. (1993) report that the
122 concentrations of $\text{R}\cdot$ and $\text{ROO}\cdot$ are time varying and depend on the radiation dose rate (D_R). To
123 interrupt oxidative reactions, antioxidants (AO) react with $\text{ROO}\cdot$ to form stable products:



125 Mason et al. (1993) indicate that consumption rate of antioxidant is related linearly to D_R :

$$126 \quad \frac{d[AO]}{dt} = -CD_R \quad (5)$$

127 where [AO] is the antioxidant concentration and C is a constant depending on properties of
128 polymer.

129

130 **MATERIALS AND METHODS**

131 **Geomembrane**

132 A commercially available 2-mm-thick smooth HDPE GM representative of GMs used in
133 LLW disposal facilities as well as thinner simulated GMs were used in this study. Properties of
134 the 2-mm-thick smooth HDPE GM are in Table 1. The simulated GMs were created by
135 mechanically pulverizing sections of 2-mm-thick smooth HDPE GM and extruding the polymer at
136 different thicknesses (e.g., 0.04, 0.1, and 0.2 mm) using a film blowing machine (Dayton Model
137 No. 6536, Dayton Manufacturing Company, Dayton, OH). **Pulverizing and extruding the
138 geomembrane had minor effect on the antioxidant concentration and the crystallinity of the
139 polymer, as described subsequently.**

140

141 **Exposure Experiments**

142 The GMs were exposed to α particles from a sealed source of ^{241}Am and β particles from
143 a sealed source of ^{99}Tc (Eckert and Ziegler, Valencia, California) (Fig. 1a, b). ^{241}Am was used as
144 a surrogate for U because of the similarity in their energy spectra. The sealed ^{241}Am source had
145 a nominal activity of 1.85 MBq with an active diameter of 9.5 mm and a peak energy of 4.7 MeV.
146 The radiation foil consisted of ^{241}Am in a gold matrix with aluminum backing. The sealed ^{99}Tc
147 source had a nominal activity of 32.3 kBq with an active diameter of 16 mm. The ^{99}Tc in the source
148 was deposited onto a plastic film covered with a 5- μm titanium foil.

149 Square GM specimens with dimensions of 21 mm x 21 mm were placed directly beneath
150 a sealed source (Fig. 1b) and exposed for 1, 5, 10, 20, or 50 hr at room temperature of 22 °C.
151 After exposure, a sample was cut from the center of the exposure area for measurement of OIT.
152 GM specimens of different thickness (0.04, 0.1, 0.2, and 2-mm-thick) were exposed to evaluate
153 depth of penetration relative to thickness of the GM.

154

155 **Oxidative Induction Time (OIT)**

156 Antioxidant depletion in the HDPE GM was characterized by OIT tests conducted in
157 accordance with ASTM D3895 using a Q100 differential scanning calorimeter (DSC) (TA
158 Instruments, Wood Dale, IL). OIT is proportional to the amount of antioxidant remaining in the
159 HDPE GM; i.e., higher OIT indicates that the GM has a greater concentration of antioxidants. OIT
160 was measured on specimens of HDPE GM before and after irradiation.

161 The initial OIT was 197 ± 5 min for the 2-mm-thick HDPE GM. For the thinner specimens,
162 the initial OIT was 185 ± 1.2 min (0.04 mm), 189 ± 1.6 min (0.1 mm), and 194 ± 0.8 min (0.2
163 mm). The similarity of the OIT data for conditions prior to radiation suggest that the grinding,
164 heating, and extrusion process had minor effect on antioxidant concentration, but the effect was
165 greater for thinner GM specimens due to their larger ratio of surface area to thickness.

166

167 **Crystallinity**

168 Crystallinity of the HDPE GM was measured using the DSC following the procedure in
169 ASTM E794. HDPE GM specimens with mass between 10 and 15 mg were sealed in an aluminum
170 pan, placed in the DSC, and then heated to 200 °C at a rate of 10 °C/min under a nitrogen
171 atmosphere. The heat of fusion was calculated by the area above the melting endotherm.
172 Crystallinity was computed as the ratio between the measured heat of fusion and the heat of
173 fusion of 100% crystalline HDPE (i.e., 290 J/g) as defined in Flory and Vrij (1963).

174 The initial crystallinity was $43.4 \pm 0.6\%$ for the 2-mm-thick HDPE GM. For the thinner
175 specimens manufactured for the study, the crystallinity was $40.5 \pm 1.1 \%$ for 0.04-mm-thick
176 specimen, $42.1 \pm 0.2 \%$ for 0.1-mm-thick specimen, and $43.0 \pm 0.1 \%$ for 0.2-mm-thick
177 specimen. Thus, the grinding, heating, and extrusion process had a minor effect on crystallinity.

178

179 Dose Deposition and Penetration Depth

180 Dose deposition and penetration depth of α and β particles in the GM specimens during
181 the sealed source experiments were **estimated** with the GEANT4 software program (Agnostinelli
182 et al. 2003). GEANT4 solves the linearized Boltzmann transport equation for particles passing
183 through user-specified geometries, and is widely used in nuclear, high-energy, and medical
184 physics (Agnostinelli et al. 2003). Energetic particles are transported according to physical
185 interactions stochastically sampled from probability distributions, with the resulting energy
186 deposition recorded in a voxelized grid. Particles are tracked until all of their kinetic energy is
187 deposited or they leave the geometry of interest (e.g., leave a GM specimen). The standard
188 physics package in GEANT4 supports simulation of radioactive isotopes, with full transport and
189 decay of all subsequent daughter products (Agnostinelli et al. 2003).

190 The sealed sources were simulated to be in direct contact with the GM specimens and
191 surrounded on all other sides by air (Fig. 1). **The GM was simulated as CH_2 with a uniform density**
192 **of 0.942 Mg/m^3 . The change of density between amorphous and crystallinity region of GM was**
193 **assumed to be negligible and not included in the model.** The GM was represented with a 41×41
194 $\times 1000$ voxel grid corresponding to a voxel size of $0.5 \text{ mm} \times 0.5 \text{ mm} \times 0.002 \text{ mm}$. The geometry
195 and activity provided by the manufacturer of each sealed source was used as input to GEANT4.
196 Peak energies predicted by GEANT4 for α and β particles were identical to those published by
197 manufacturer of the sealed sources, indicating that the GEANT4 simulations represented the
198 transport of α and β particles from the sealed sources reliably. **Each GEANT4 model simulated**

199 10,000,000 single decay events and integrated the total energy deposition. Dose per decay was
200 computed by normalizing total energy deposition profile.

201

202 **RESULTS AND DISCUSSION**

203 **Antioxidant Depletion for Sealed Source Experiments**

204 OIT as a function of exposure time for the HDPE GM is shown in Fig. 2. OIT decreased
205 faster for the thinner specimens. For example, OIT of the 0.1-mm-thick GM decreased from 189
206 min to 177 min after exposure to ^{241}Am for 50 h (Fig. 2a), whereas OIT of the 0.2-mm-thick
207 specimen decreased from 194 min to 189 min with the same exposure. Exposure to β radiation
208 had a similar effect (Fig. 2b), except the depletion rate was greater for α exposure (^{241}Am) relative
209 to β exposure (^{99}Tc) due to the lower activity of the ^{99}Tc sealed source. For example, OIT of the
210 0.04-mm-thick GM decreased from 185 to 174 min after exposure to ^{99}Tc for 50 h (Fig. 2b),
211 whereas exposure to ^{241}Am for 50 h resulted in OIT decreasing from 185 to 158 min for 0.04-mm-
212 thick GM (Fig. 2a).

213 Depletion of antioxidants occurs when α and β particles break C-C or C-H bonds (Phillips
214 1988, Whyatt and Farnsworth 1990, Mason et al. 1993, Costa et al. 2008). The antioxidants
215 protect the HDPE GM from degradation by reacting with free radicals that form when the C-C or
216 C-H bonds are broken (Hsuan and Koerner 1998, Gulec et al. 2004). Depletion of OIT diminishes
217 as the thickness of the HDPE GM increases (e.g., 0.2-mm-thick and 2-mm-thick), indicating that
218 the α and β particles have less impact as the depth of penetration diminishes relative to the
219 thickness of the GM. Areas close to the source are expected to have greater antioxidant depletion,
220 and those farther away less depletion.

221 GEANT4 was used to simulate dose deposition and particle penetration for the sealed
222 source experiments as a function of depth in the GM. Predictions of dose deposition per decay
223 from the GEANT4 simulation at the center of exposed area of the HDPE GM are shown in Fig. 3

224 for ^{241}Am (α , Fig. 3a) and ^{99}Tc (β , Fig. 3b). The peak dose at the surface of the GM was predicted
225 as 2.2×10^{-7} Gy per decay from ^{241}Am and 5.2×10^{-10} Gy per decay from ^{99}Tc . For both sources,
226 the dose decreases with depth and becomes negligible at 28 μm (α , Fig. 3a) or 0.48 mm (β , Fig.
227 3b). Exposure time does not affect the maximum penetration depth, which is controlled by the
228 peak energy of the particle (approximately 4.7 MeV for α particle, 294 keV for β particle) provided
229 that the density and composition of the exposed material does not change significantly.

230 These findings suggest that the HDPE GM is not affected by α particles from the ^{241}Am at
231 distances greater than 28 μm from the sealed source. For β particles from the ^{99}Tc , the distance
232 is 0.48 mm. Consequently, the impact of radiation on the overall GM diminishes as the GM
233 becomes thicker. Radiation from α particles affects approximately 70% of the 0.04-mm-thick
234 HDPE GM specimen, 28% of the 0.1-mm-thick specimen, 14% of the 0.2-mm-thick specimen,
235 and only 1.4% of the 2-mm-thick specimen. Similarly, β radiation affects 100% of the 0.04-mm-,
236 0.1-mm-, and 0.2-mm-thick HDPE GMs, and only 24% of the 2-mm-thick specimen.

237

238 **Predicting Antioxidant Depletion**

239 The OIT measurement reflects the aggregate impact of antioxidants in all areas of the GM,
240 and therefore represents an average reduction in antioxidant concentration. In reality, antioxidant
241 depletion is depth dependent, with decreasing depletion as the distance from the radiation source
242 increases. Measuring the variation in OIT within the thin specimens was not possible with the
243 resources available. Thus, to estimate the depth dependence, a multilayer model was created
244 where the HDPE GM is divided into a series of layers of equal thickness, with a uniform dose
245 applied to each layer (Fig. 4). Those layers within the depth of penetration of α or β particles have
246 non-zero dose and are defined as comprising the “impacted zone” (Fig. 4). Layers outside the
247 depth of penetration have zero dose and comprise the “unimpacted zone.” The impacted zone is
248 thicker for β radiation (Fig. 3b) than α radiation (Fig. 3a) because β particles penetrate deeper in
249 the GM (Fig. 3b) than α particles.

250 Antioxidant concentration in the i^{th} layer with dose deposition ($D_{i(z,t)}$) is assumed to follow
 251 the relationship in Mason et al. (1993):

$$252 \quad [AO]_i = [AO]_0 - kD_{i(z,t)} \quad (6)$$

253 where $[AO]_0$ is the initial antioxidant concentration (before irradiation), $[AO]_i$ is the antioxidant
 254 concentration after receiving $D_{i(z,t)}$, and k is a depletion coefficient that depends on the antioxidant
 255 package and type of radiation. The dose $D_{i(z,t)}$ is a function of depth from the surface (z) and
 256 exposure time (t). **By mass conservation**, the average antioxidant concentration in the GM after
 257 exposure, $[AO]_{\text{ave}}$, is the arithmetic mean of $[AO]_i$ in each layer:

$$258 \quad [AO]_{\text{ave}} = \frac{\sum_i^n ([AO]_0 - kD_{i(z,t)})}{n} \quad (7)$$

259 where n represents the number of layers in the HDPE specimen. Mason et al. (1993) indicate
 260 that OIT is related exponentially to antioxidant concentration:

$$261 \quad \text{OIT}_{[AO]} = \delta e^{\theta[AO]} \quad (8)$$

262 where $\text{OIT}_{[AO]}$ is the OIT with $[AO]$ in the specimen, **δ is a material-dependent constant, and θ**
 263 **is an antioxidant concentration constant that is unique to each antioxidant package. Combining**
 264 **Eqs. 7 and 8 yields the average OIT $\{\text{OIT}_{[AO]_{\text{ave}}}\}$ of the GM as a function of the initial OIT $\{\text{OIT}_{[AO]_0}\}$**
 265 **corresponding to the initial AO concentration $\{[AO]_0\}$ and the depth dependent distribution of**
 266 **dose $[D_{i(z,t)}]$:**

$$267 \quad \text{OIT}_{[AO]_{\text{ave}}} = \text{OIT}_{[AO]_0} e^{-k^* \sum_i^n \frac{D_{i(z,t)}}{n}} \quad (9)$$

268 where k^* ($=\theta k$) is the effective radiation depletion coefficient and represents the original
 269 antioxidant concentration and the antioxidant package [units for k^* are in $\ln(\text{min})/\text{Gy}$]. The
 270 parameter δ in Eq. 8 is implicit in $\text{OIT}_{[AO]_0}$ in Eq. 9. Linearization of Eq. 9 yields:

271
$$\ln(\text{OIT}_{[\text{AO}]_{\text{ave}}}) = \ln(\text{OIT}_{[\text{AO}]_0}) - k^* \left(\sum_i^n \frac{D_{i(z,t)}}{n} \right) \quad (10)$$

272 Eq. 10 was fit to the OIT data from the sealed source experiments using simultaneous
 273 linear least-squares regression with $n = 1000$. The doses $[D_{i(z,t)}]$ in Eq. 10 **used in each fit were**
 274 computed as the product of the normalized dose-per-decay (Fig. 3) and the exposure time-
 275 integrated activity of each sealed source. These fits are shown in Fig. 5. **A step-by-step example**
 276 **of the calculation procedure is in the Appendix.** The fit of Eq. 10 is better for thicker specimens ($>$
 277 0.1 mm), which may be due to uncertainty in the thickness of the thinner GMs. The caliper used
 278 to measure GM thickness had a precision of 0.02 mm, leading to the greater uncertainty in
 279 thickness for the specimen as the thickness decreased.

280 **Eq. 10 was checked by estimating OIT of the 0.1, 0.2, and 2.0-mm-thick HDPE specimens**
 281 **for 50 hr of exposure to ^{241}Am using k^* obtained by fitting Eq. 10 only to the OIT data for the 0.04-**
 282 **mm-thick specimen. The dose deposition profile from GEANT4 for a 0.04-mm-thick specimen was**
 283 **used as $D_{i(z,t)}$ when fitting Eq. 10 to the OIT data. For the estimates of OIT, the dose deposition**
 284 **from GEANT4 used in Eq. 10 corresponded to 0.1, 0.2, and 2.0-mm-thick HDPE specimens. As**
 285 **shown in Fig. 6, good agreement exists between the estimated and measured OIT after 50 hr of**
 286 **exposure, regardless of thickness, when parameterized using only the data from tests conducted**
 287 **on 0.04-mm-thick specimens.**

288 OIT **estimated** with the multilayer model as a function of depth is shown in Fig. 7 for 0.2-
 289 mm-thick HDPE specimens exposed to α (Fig. 7a) and β (Fig. 7b) radiation for up to 50 h. For α
 290 radiation, OIT depletion is largest at the surface of HDPE GM due to the high radiation dose at
 291 the surface, and diminishes rapidly with depth until the maximum depth of penetration is reached
 292 at 28 μm (depth of impacted zone, Figs. 3 and 4). Beyond this depth, no change in OIT is
 293 **estimated** due to radiation, although other mechanisms could contribute to antioxidant depletion
 294 in an actual application. For β radiation, the dose is greatest at the surface but spans the entire

295 thickness (Fig. 3). Consequently, antioxidant depletion is greatest at the surface, but extends
296 throughout the entire thickness because of the greater penetration of β particles (Fig. 7b). As the
297 exposure time increases, greater OIT depletion occurs in the impact zone for both α and β
298 particles. The depth of the impact zone, however, remains constant at the maximum depth of
299 penetration.

300

301 PRACTICAL IMPLICATIONS

302 Dose Expected in LLW Liner Application

303 GEANT4 was used to estimate doses that would be realized in the field for a composite
304 liner overlain by LLW leachate. The conceptual model was similar to that used for interpreting the
305 sealed-source experiments, and included three layers: a thin (10 mm) layer of leachate, a 2-mm-
306 thick HDPE geomembrane, and a 100-mm-thick soil layer representing a geosynthetic clay liner
307 over an attenuation layer (Fig. 8). The leachate was assumed to be water (density = 1.0 Mg/m³),
308 the GM was assumed to be CH₂ with a density of 0.942 Mg/m³, and the soil layer was
309 approximated as SiO₂ with a density of 1.8 Mg/m³. Thickness of the leachate layer was chosen
310 as 10 mm due to limited depth of penetration of α and β particles in water. The GM layer was
311 represented to a 21 × 21 × 1000 voxel grid, with a voxel size of 10 mm × 10 mm × 0.002 mm.

312 Radioactive source particles were simulated with a uniform distribution within the leachate.
313 The U concentration was assumed to be 1500 μ g/L as reported in Tian et al. (2017b), with ²³⁴U,
314 ²³⁵U, and ²³⁸U in their natural abundance. The ⁹⁹Tc concentration was simulated to be 29.6 Bq/L
315 as reported in Tian et al. (2017b). Total dose was computed as the product of the normalized
316 dose-per-decay and the 1000 yr time-integrated activity of each isotope.

317 Dose profiles in the GM for ²³⁴U, ²³⁵U, ²³⁸U, and ⁹⁹Tc as well as their combined dose for
318 the 1000-yr service life are shown in Fig. 9. The peak dose is 2.42 Gy at the surface, with α -
319 particles from U comprising the majority of the dose. ²³⁴U contributes 1.21 Gy and ²³⁸U contributes
320 1.15 Gy. ²³⁵U and ⁹⁹Tc contribute the remaining 0.06 Gy. The rapid decrease in dose between 0.0

321 and 0.07 mm corresponds to the maximum penetration of α particles emitted from U (4.27–4.86
322 MeV) and its daughter products (e.g., 4.68 MeV for ^{230}Th , 4.60 for ^{226}Ra , and 7.68 MeV for ^{214}Po)
323 in the full decay chain. The dose from β radiation emitted from ^{99}Tc reaches approximately 0.5
324 mm, but is much smaller due to the lower activity and peak energy of ^{99}Tc . The profiles of U also
325 exhibit a small dose throughout the entire thickness due to β or γ radiation emitted from daughter
326 isotopes. Some of daughter isotopes have a very long half-life (e.g., 75,380 yr for ^{230}Th).

327 Doses in an actual HDPE GM in a LLW containment system may be lower due to
328 simplifying assumptions in the GEANT4 model. For example, nonwoven geotextiles are normally
329 deployed on top of HDPE GMs as a protective layer, and leachate will be in the pores of a granular
330 leachate collection system (LCS) on top of the GM. The geotextile and the LCS will shield the
331 radiation, resulting in a lower dose to the GM. Consequently, the dose deposition predicted by
332 the GEANT4 model probably is an overestimate for an actual liner configuration.

333

334 **Antioxidant Depletion**

335 OIT in the GM at 1000-yr was **estimated** as a function of depth using the multilayer model
336 and the α and β dose profiles in Fig. 9. At 1000 yr, OIT at the surface of GM would decrease less
337 than 0.01 min due to α radiation emitted from U (Fig. 10a) and less than 0.2 min due to β radiation
338 emitted from ^{99}Tc (Fig. 10b). Given that the initial OIT of the HDPE GM is 197 min, the depletion
339 of antioxidants due to α and β radiation from LLW leachate would be negligible over the 1000-yr
340 service life, and is likely much smaller than depletion from other mechanisms (antioxidant
341 leaching, conventional oxidation, oxidation catalyzed by metals) (Tian et al. 2014, 2017a). The
342 actual OIT depletion due to radiation may be even lower due to the aforementioned simplifying
343 assumptions in the model.

344 These computations were based on radionuclide concentrations in leachate in existing
345 DOE on-site disposal facilities that employ waste acceptance criteria (WAC) to ensure adequately
346 low doses to receptors. If these WAC were less stringent, however, the activity in the leachate

347 could increase, resulting in a higher dose and potentially greater antioxidant depletion. To
348 evaluate this scenario, the dose was assumed to be 10x or 100x higher than the current equivalent
349 dose over 1000 yr. The **estimated** impact of these higher doses on antioxidant depletion in the
350 HDPE GM is also shown in Fig. 10.

351 The increase in α radiation results in a decrease in OIT < 0.5 min for a 100x higher dose,
352 which is much smaller than the OIT depletion likely to occur due to other mechanisms (Tian et al.
353 2017a) over 1000 yr. Increasing the β dose by 100x higher leads to a larger (20 min) decrease of
354 OIT at the surface of HDPE GM, which is approximately 10% of the initial OIT, but is still
355 considerably smaller than the depletion of OIT expected by other mechanisms. Thus, less
356 stringent WAC are unlikely to have a significant impact on **antioxidant depletion** of HDPE GMs in
357 LLW disposal facilities. **However, the combined impact of radiation and other degradation**
358 **mechanisms (e.g., oxidation degradation, thermal degradation) will accelerate the rate of**
359 **decomposition of HDPE GM beyond that shown in Fig. 10. The overall degradation cannot be**
360 **predicted based on the impacts of radiation alone.**

361

362 **SUMMARY AND CONCLUSIONS**

363 The effect of α and β radiation on antioxidant depletion was investigated for a high-density
364 polyethylene (HDPE) geomembrane (GM) used for liners in low-level radioactive waste (LLW)
365 disposal facilities. Specimens of HDPE GMs were exposed to sealed sources of ^{241}Am and ^{99}Tc
366 for 1–50 h to simulate α and β radiation from LLW. OIT tests were conducted on the specimens
367 after irradiation to examine antioxidant depletion. Dose deposition and depth of penetration of α
368 and β particles in HDPE GMs were predicted using the GEANT4 software program, which is used
369 to predict particle migration through matter in nuclear and medical physics. A multilayer analytical
370 model was created to **estimate** antioxidant depletion in HDPE GMs as a function of dose
371 deposition, and to **estimate** antioxidant depletion in a field scenario where a GM is used in a
372 composite liner in a LLW disposal facility.

373 The following conclusions are drawn from this study:

- 374 • Antioxidant depletion in HDPE GMs increases with increasing exposure to α and β radiation,
375 but is highly sensitive to the thickness of the GM. Larger increases in antioxidant depletion
376 occur in thinner GMs. Radiation by α and β particles had negligible impact on antioxidant
377 depletion in the 2-mm-thick HDPE GM used in this study.
- 378 • **Estimates obtained** with the GEANT4 program illustrate that α particles from a sealed source
379 of ^{241}Am carrying 4.7 MeV penetrate approximately 28 μm into a 2-mm-thick HDPE GM, and
380 β particles from ^{99}Tc carrying 294 keV penetrate approximately 0.48 mm. The shallow
381 penetration **estimated** with GEANT4 is consistent with the sensitivity of antioxidant depletion
382 to GM thickness measured in this study. The GEANT4 simulations showed that dose
383 deposition of α and β radiation is highest at the surface, and drops rapidly with increasing
384 depth into the GM (more rapidly for α relative to β).
- 385 • **Estimates obtained** with the GEANT4 program illustrate that α particles from U (e.g.,
386 penetration depth < 0.7 μm) and β particles from ^{99}Tc (e.g., penetration depth < 0.5 mm) in
387 LLW leachate will predominantly affect only the surface of a typical 2-mm-thick HDPE GM.
388 The total dose at the surface is on the order of 2.4 Gy over a 1000-yr period for typical LLW
389 leachate, and diminishes more than an order of magnitude within 0.1 mm from the surface of
390 the GM. **Estimates** of antioxidant depletion for these doses made using the multilayer
391 analytical model indicate that OIT depletion due to α radiation from LLW leachate is likely to
392 be less than 0.1 min (initial OIT = 197 min) over 1000 yr, and less than 1 min from β radiation.
393 This suggests that radiation from LLW is unlikely to have a significant effect on the service life
394 of GMs relative to other physical and chemical mechanisms.
- 395 • The multilayer model was used to evaluate how increasing doses due to less restrictive waste
396 acceptance criteria might affect antioxidant depletion. Increasing the dose by 100x caused a

397 decrease in OIT from 197 min to 177 min over 1000 yr. While not insignificant, this loss of
398 antioxidants is much less than anticipated due to other mechanisms over 1000 yr.

399

400 **ACKNOWLEDGEMENT**

401 Financial support for this study was provided by the US Department of Energy (DOE)
402 under cooperative agreement DE-FC01-06EW07053 entitled the “Consortium for Risk Evaluation
403 with Stakeholder Participation III.” GSE Inc. provided the geomembrane used in this study.

404

405 **APPENDIX**

406 The following illustrates how the multilayer model is used to predict the impact of radiation
407 on antioxidant depletion in an HDPE GM. The analysis consists of three steps.

408

409 **Step 1: Obtain dose per decay in each sublayer of HDPE GM**

410 For the multilayer model, a HDPE GM is discretized into n sublayers of equal thickness.
411 For the estimates made in this study, n = 1000 and the total thickness of the GM is 2 mm
412 corresponding to a sublayer thickness = 2 μm. The dose in each sublayer is assigned from the
413 dose deposition curves predicted by GEANT4 for α or β radiation. The average dose per decay
414 ($D_{i\text{-per decay}}$) in each sublayer is obtained from the dose deposition profile as shown in Fig. A1:

$$415 \quad D_{i\text{-per decay}} = \frac{D_{i\text{-top}} + D_{i\text{-bot}}}{2} \quad (A1)$$

416 where $D_{i\text{-top}}$ is dose per decay at the top of the i^{th} layer, $D_{i\text{-bot}}$ is dose per decay at the bottom of the
417 i^{th} layer, and $D_{i\text{-per decay}}$ is the dose per decay assigned to the i^{th} layer. For example, for the 6th layer
418 (depth = 0.010 to 0.012 mm), the dose in the HDPE GM at depth of 0.010 mm is 1.3×10^{-7} Gy
419 and at 0.012 mm the dose is 9.4×10^{-8} Gy. Thus, the average dose deposition per decay in the
420 6th layer is 1.12×10^{-7} Gy.

421

422 **Step 2: Calculate dose deposition in HDPE GM after exposure**

423 Step 1 yields the dose deposited per decay of the radiation source. Total dose deposition
424 in layer i of an HDPE GM [$D_{i(z,t)}$] over a period of time is the summation of these doses over time.
425 The total dose is computed as the product of the dose per decay at a given depth (z) (Fig. A1),
426 the source activity, and the exposure time (t).

427
$$D_{i(z,t)} = D_{i\text{-per decay}} \times \text{activity} \times \text{time} \quad (\text{A2})$$

428 For example, the total dose deposited in the 6th layer after 1 hr of exposure can be calculated as:

429
$$D_{6(0.11\text{mm},1\text{hr})} = 1.12 \times 10^{-7} \frac{\text{Gy}}{\text{decay}} \times 1.85 \times 10^6 \frac{\text{decay}}{\text{s}} \times 3600\text{s} = 746\text{Gy}$$

430

431 **Step 3: Determine radiation depletion coefficient**

432 The effective radiation depletion coefficient k^* is obtained regressing Eq. 10 on OIT data from
433 sealed source experiments using the doses computed in Step 2 as follows:

434
$$\ln(\text{OIT}_t) = \ln(\text{OIT}_0) - \frac{k^*}{n} \sum_{i=1}^n D_{i(z,t)} \quad (\text{A3})$$

435 In Eq. A3, OIT_t is the OIT measured on a specimen exposed for exposure time t in a sealed source
436 experiment, OIT_0 is the initial OIT of the GM prior to irradiation, and $D_{i(z,t)}$ corresponds to the doses
437 in the sublayers of the specimen computed using the procedure in Step 2. An example is shown
438 in Fig. A2 for data from sealed source experiments conducted with ²⁴¹Am for 1, 5, 10, 20, and 50
439 hr on 0.2 mm-thick specimens with the OIT determined by DSC. Eq. A3 is regressed
440 simultaneously on data from sealed source experiments on specimens of various thickness (0.04,
441 0.1, 0.2, and 2 mm in this study) to obtain a single k^* for the source, GM polymer, and antioxidant

442 package. From the regression shown in Fig. A2, $k^* = 7.12 \times 10^{-6}$ [units = ln(min)/Gy] for α radiation
443 for the dose from ^{241}Am in Gy and OIT in minutes.

444

445 REFERENCES

446 Abdelaal, F., and Rowe, K. (2015). Effect of high pH found in low-level radioactive waste leachates
447 on the antioxidant depletion of a HDPE geomembrane. *Journal of Hazardous, Toxic, and*
448 *Radioactive Waste*, 10.1061/(ASCE)HZ.2153-5515.0000262, D4015001.

449 Agnostinelli, S. et al. (2003). GEANT4-a simulation toolkit. *Nuclear Instruments and Methods in*
450 *Physics Research A*, Vol. 506, 250–303.

451 ASTM D4218 (2015). Standard test method for determination of carbon black content in
452 polyethylene compounds by the muffle-furnace technique, Annual Book of Standards, Vol
453 08.02, ASTM International, West Conshohocken, PA.

454 ASTM D5885 (2015). Standard test method for oxidative induction time of polyolefin
455 geosynthetics by high-pressure differential scanning calorimetry, Annual Book of Standards,
456 Vol 04.13, ASTM International, West Conshohocken, PA.

457 ASTM D3895 (2014). Standard test method for oxidative-induction time of polyolefins by
458 differential scanning calorimetry, Annual Book of Standards, Vol 08.02, ASTM International,
459 West Conshohocken, PA.

460 ASTM D1238 (2013), Standard test method for melt flow rates of thermoplastics by extrusion
461 plastometer, Annual Book of Standards, Vol 08.01, ASTM International, West Conshohocken,
462 PA.

463 ASTM E794 (2012). Standard test method for melting and crystallization temperatures by thermal
464 analysis, Annual Book of Standards, Vol 14.05, ASTM International, West Conshohocken, PA.

465 ASTM D5199 (2012). Standard test method for measuring the nominal thickness of geosynthetics,
466 Annual Book of Standards, Vol 04.13, ASTM International, West Conshohocken, PA.

467 ASTM D1505 (2010). Standard test method for density of plastics by the density-gradient
468 technique, Annual Book of Standards, Vol 08.01, ASTM International, West Conshohocken,
469 PA.

470 Czvikovszky, T. (2004) Degradation effects in polymers. *In: IAEA-TECDOC-1420 Advances in*
471 *radiation chemistry of polymers*. Proceedings of a technical meeting held in Notre Dame,
472 Indiana, International Atomic Energy Agency. Vienna, Austria.

473 Costa, L., Carpentieri, I., and Bracco, P. (2008). Post electron-beam irradiation oxidation of
474 orthopaedic UHMWPE. *Polymer Degradation and Stability*, 93(9), 1695–1703.

475 DOE (2001). Radioactive Waste Management, Order 435.1, U. S. Department of Energy,
476 Washington DC.

477 Gulec, S., Edil, T., and Benson, C. (2004) Effect of acidic mine drainage on the polymer properties
478 of an HDPE geomembrane. *Geosynthetics International*, 11(2), 60–72.

479 Grassie, N., and Scott, G. (1985). *Polymer Degradation and Stabilization*. Cambridge University
480 Press, New York, USA.

481 Hsuan, Y., and Koerner, R. (1998). Antioxidant depletion lifetime in high density polyethylene
482 geomembranes. *Journal of Geotechnical and Geoenvironmental Engineering*, 124(6), 532–
483 541.

484 Mason, L., Doyle, T., and Reynolds, A. (1993). Oxidation induction time correlations with radiation
485 dose and antioxidant concentration in EPR and XLPE Polymers. *Journal of Applied Polymer*
486 *Science*, Vol. 50, 1493–1500.

487 Osawa, Z., and Ishizuka, T. (1973) Catalytic action of metal salts in autoxidation and
488 polymerization. *Journal of Applied Polymer Science*, 17, 2897–2907.

489 Peacock, A. (2000). *Handbook of Polyethylene: Structures, Properties and Application*. Marcel
490 Dekker Inc., New York, (2000).

491 Phillips, D. (1988). Effect of radiation on polymers. *Materials Science and Technology*, 4, 85–91.

492 Powell, J., Abitz, R., Broberg, K., Hertel, W., and Johnston, F. (2011). Status and performance of
493 the On-Site Disposal Facility, Fernald Preserve, Cincinnati, Ohio. Paper 11137, *Proceedings*
494 *Waste Management '11*, WM Symposia Inc., Phoenix, AZ.

495 Rowe, R., Abdelaal, F., and Brachman, R. (2013). Antioxidant depletion of HDPE geomembrane
496 with sand protection layer. *Geosynthetics International*, 20(1), 73–89.

497 Rowe, R., Islam, M., Brachman, R., Arnepalli, D., and Ewais, A. (2010). Antioxidant depletion
498 from a high-density polyethylene geomembrane under simulated landfill conditions. *Journal*
499 *of Geotechnical and Geoenvironmental Engineering*, 136(7), 930–939.

500 Rowe, R., Rimal, S., and Sangam, H. (2009). Ageing of HDPE geomembrane exposed to air,
501 water and leachate at different temperatures. *Geotextiles and Geomembranes*, 27, 137–151.

502 Rowe, R., and Rimal, S. (2008). Depletion of antioxidants from an HDPE geomembrane in a
503 composite liner. *Journal of Geotechnical and Geoenvironmental Engineering*, 134(1), 68–78.

504 Rowe, R., Islam, M., and Hsuan, Y. (2008). Leachate chemical composition effects on OIT
505 depletion in an HDPE geomembrane. *Geosynthetics International*, 15(2), 136–151.

506 Rowe, R. and Sangam, H. (2002). Durability of HDPE geomembranes. *Geotextiles and*
507 *Geomembranes*, 20, 77–95.

508 Sangam, H., and Rowe, R. (2002). Effects of exposure conditions on the depletion of antioxidants
509 from high-density polyethylene (HDPE) geomembrane. *Canadian Geotechnical Journal*, 39,
510 1221–1230.

511 Tian, K., Benson, C., Tinjum, J., and Edil, T. (2017a). Antioxidant depletion and service life
512 prediction for HDPE Geomembranes exposed to low-level radioactive waste leachate. *Journal*
513 *of Geotechnical and Geoenvironmental Engineering*, 10.1061/(ASCE)GT.1943-
514 5606.0001643.

515 Tian, K, Benson, C., Tinjum, J. (2017b). Chemical characteristics of leachate in low-level
516 radioactive waste disposal facilities. *Journal of Hazardous, Toxic, and Radioactive Waste*,
517 10.1061/(ASCE)HZ.2153-5515.0000361.

518 Tian, K., Benson, C., and Likos, W. (2016a). Hydraulic conductivity of geosynthetic clay liners to
519 low-level radiative waste leachate. *Journal of Geotechnical and Geoenvironmental*
520 *Engineering*, 10.1061/(ASCE)GT.1943-5606.0001495, 04016037.

521 Tian, K., Yang, Y., Benson, C., and Tinjum, J. (2015). Effect of low-level radioactive waste
522 leachate on antioxidant depletion in HDPE geomembranes. *Proceedings Waste Management*
523 *15*, WM Symposia Inc., Phoenix, AZ.

524 Tian, K., Tinjum, J., Benson, C., and Edil, T. (2014) Antioxidant depletion in HDPE
525 geomembranes exposed to low-level radioactive waste leachate. *Geo-Congress 2014, Geo-*
526 *Characterization and Modeling for Sustainability*, GSP 234, Edited by Abu-Farsakh, M., Yu,
527 X., and Hoyos, L., ASCE, Reston, VA, 1816-1825.

528 Tian, K. (2012). Durability of high-density polyethylene geomembrane in low-level radioactive
529 waste leachate. *MS Thesis*, Univ. of Wisconsin-Madison, Madison, Wisconsin.

530 Turner, J. (2007). *Atoms, Radiation, and Radiation Protection*. WILEY-VCH Verlag GmbH & Co.
531 KGaA, Weinheim.

532 Whyatt, G. and Farnsworth, R. (1990). The high pH chemical and compatibility of various liner
533 materials. *Geosynthetic Testing for Waste Containment Applications, STP 1081*, R. Koerner,
534 editor, ASTM International, West Conshohocken, PA, 110-124.

LIST OF TABLES AND FIGURES

Table 1. Properties of HDPE GM used in Sealed Source Experiments.

- Fig. 1. Set up for sealed-source experiments: (a) sealed sources of ^{99}Tc (left) and ^{241}Am (right) and (b) GM installed under the sealed source for exposure. Divisions on scale in (a) are in mm.
- Fig. 2. OIT vs. exposure time for HDPE GM specimens exposed to sealed sources of ^{241}Am (a) and ^{99}Tc (b) for up to 50 h. Error bars represent standard deviation of three measurements
- Fig. 3. Dose per decay as a function of depth from the surface of the GM predicted by GEANT4 for HDPE GM exposed to a sealed source of ^{241}Am (a) or ^{99}Tc (b).
- Fig. 4. Layering in multilayer model for antioxidant depletion in HDPE GM exposed to radiation with antioxidant concentration $[\text{AO}]_i$ after exposure to radiation dosage D_i . Each layer in un-impacted zone (no dose) has the initial antioxidant concentration $[\text{AO}]_0$.
- Fig. 5. Fit of Eq. 10 to obtain k^* using OIT data for 0.04, 0.1, 0.2, and 2-mm-thick HDPE GM specimens after exposure to sealed sources of ^{241}Am (a) and ^{99}Tc (b) for up to 50 h. Fit made using simultaneous regression on data from all specimens.
- Fig. 6. Comparison of predicted and measured OIT for 0.04, 0.1, 0.2, and 2-mm-thick HDPE specimens using k^* from OIT data from 0.04-mm-thick specimen as input (solid symbols) or k^* from simultaneous regression. Dose deposition defined by GEANT4.
- Fig. 7. OIT as a function of depth from surface of GM computed using multilayer model for 0.2-mm-thick HDPE GM exposed to sealed source of ^{241}Am (a) or sealed source of ^{99}Tc (b).
- Fig. 8. Domain simulated with GEANT4 representing composite liner with HDPE GM on compacted clay liner with thin layer of LLE leachate pooled above. LLW leachate assumed to contain radionuclides and major cations and anions in Table 2 based on the leachate characterization reported in Tian et al. (2016, 2017a).
- Fig. 9. Dose as function of depth in HDPE GM in a composite liner overlain with LLW leachate after 1000 yr of exposure as predicted with GEANT4.
- Fig. 10. OIT as a function of depth in HDPE GM exposed to α (a) and β (b) radiation for 1000 yr for base case and doses 10x and 100x higher than dose for base case.
- Fig. A1. Dose per decay as a function of depth from the surface of the GM predicted by GEANT4 for HDPE GM exposed to a sealed source of ^{241}Am .
- Fig. A2. Fit of multilayer model Eq. A3 (solid line) to OIT data for 0.2-mm-thick HDPE GM specimens after exposure to sealed sources of ^{241}Am for up to 50 h.

Table 1. Properties of HDPE GM used in Sealed Source Experiments.

Property	ASTM Method	Average
Density (kg/m ³)	D1505	946
Average Thickness (mm)	D5199	2.0
Carbon black content (%)	D4218	2.62
Standard Oxidation Induction Time (min)	D3895	197
High-Pressure Oxidation Induction Time (min)	D5885	831
Crystallinity (%)	E794	43.4
Melt Flow Index (g/10 min)	D1238	0.08

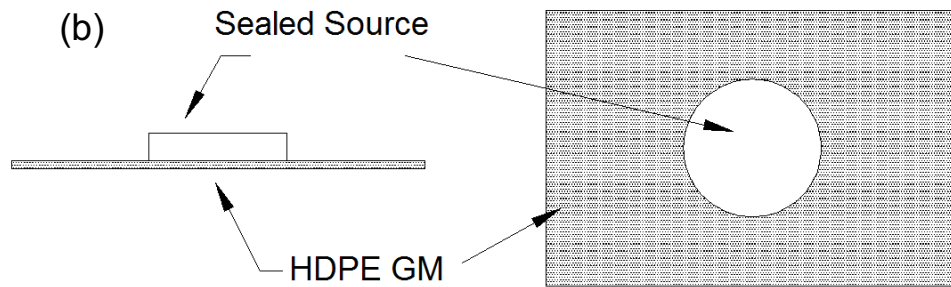
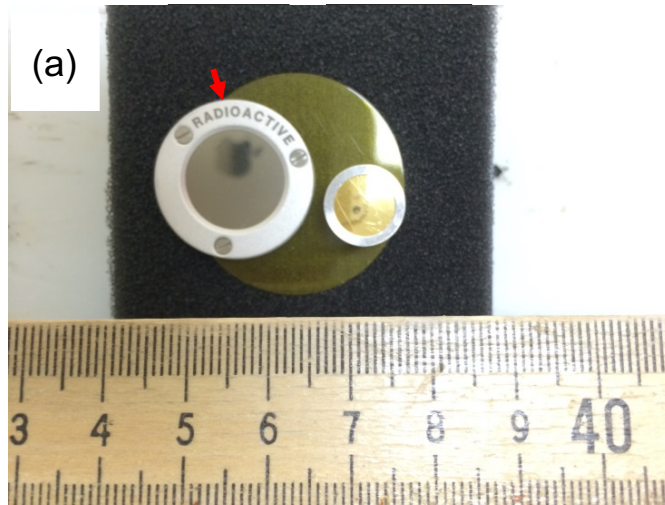


Fig. 1. Set up for sealed-source experiments: (a) sealed sources of ^{99}Tc (left) and ^{241}Am (right) and (b) GM installed under the sealed source for exposure. Divisions on scale in (a) are in mm.

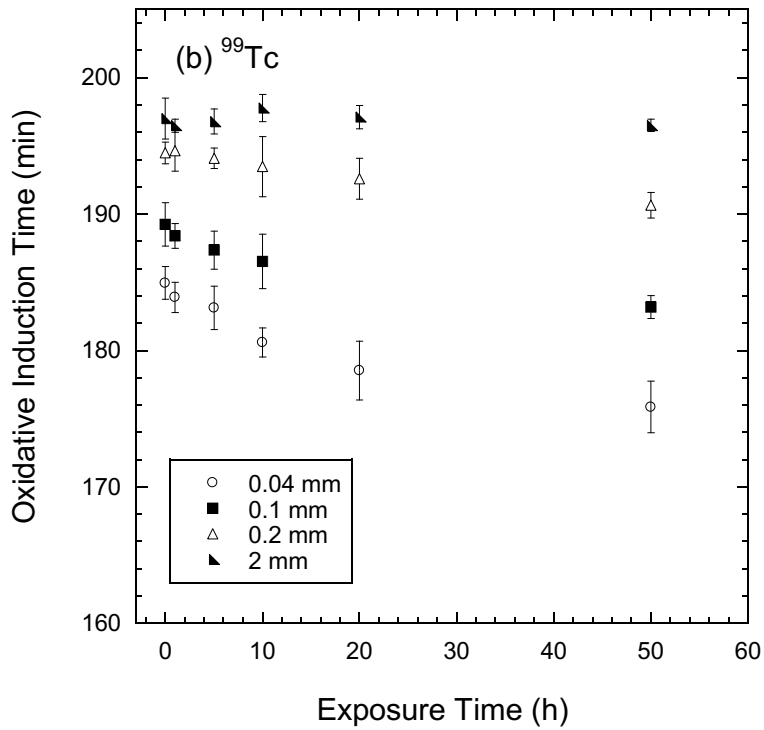
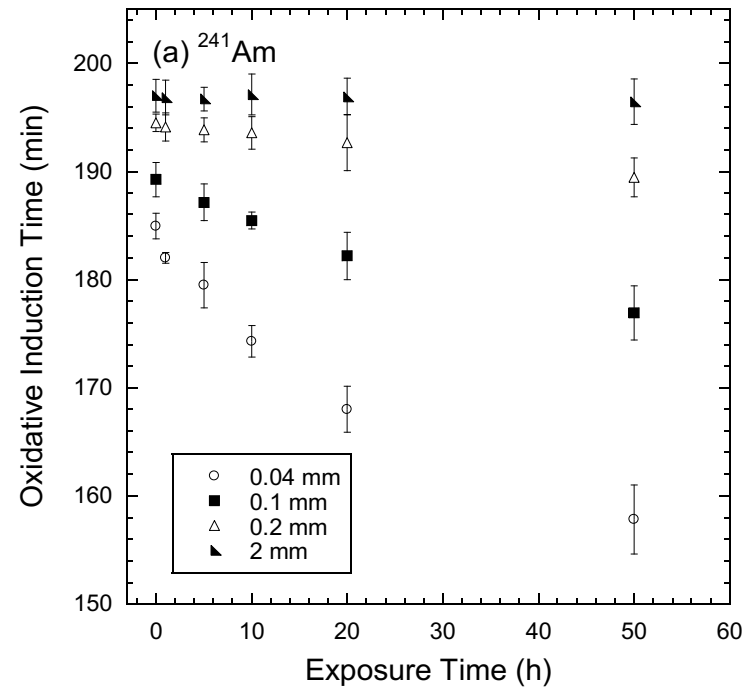


Fig. 2. OIT vs. exposure time for HDPE GM specimens exposed to sealed sources of ^{241}Am (a) and ^{99}Tc (b) for up to 50 h. Error bars represent standard deviation of three measurements.

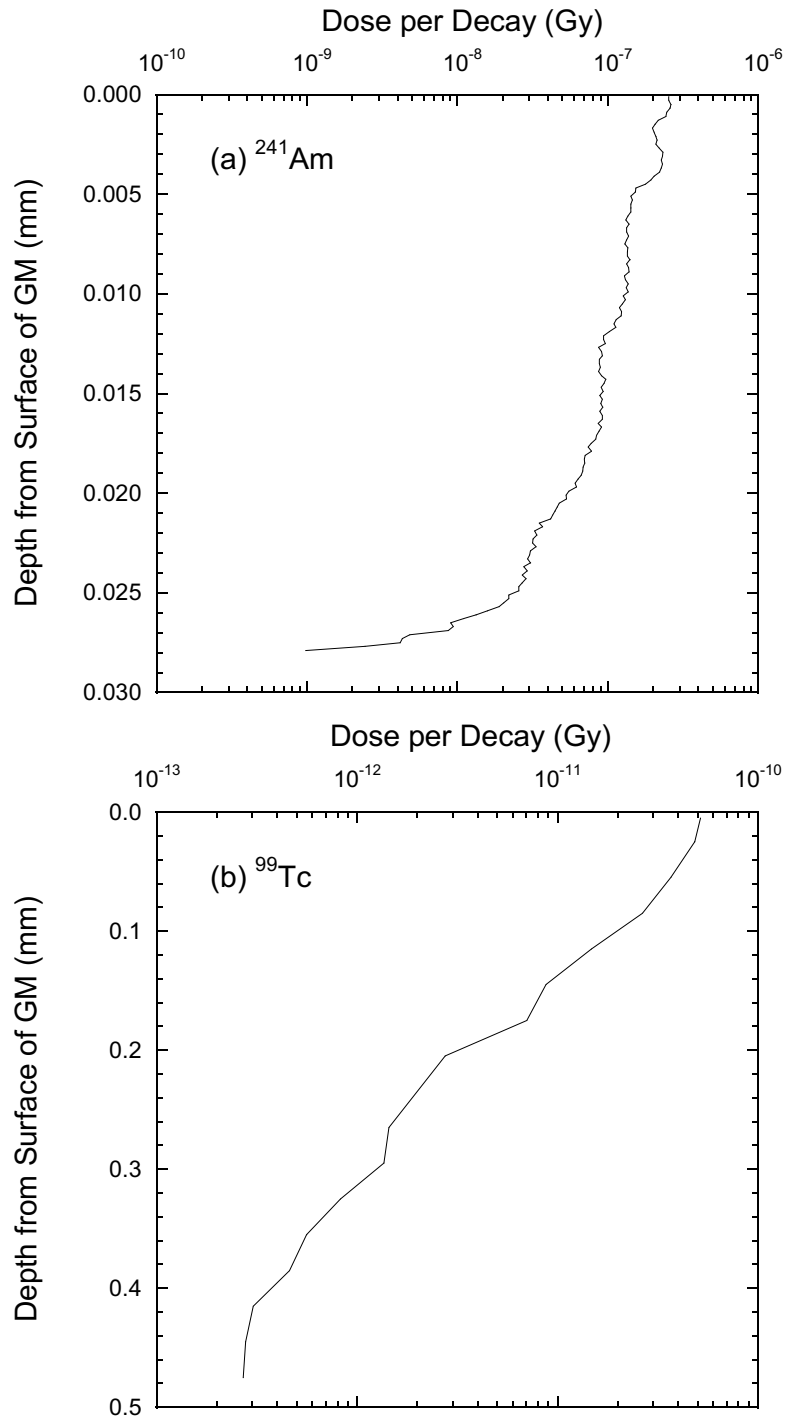


Fig. 3. Dose per decay as a function of depth from the surface of the GM predicted by GEANT4 for HDPE GM exposed to a sealed source of ^{241}Am (a) or ^{99}Tc (b).

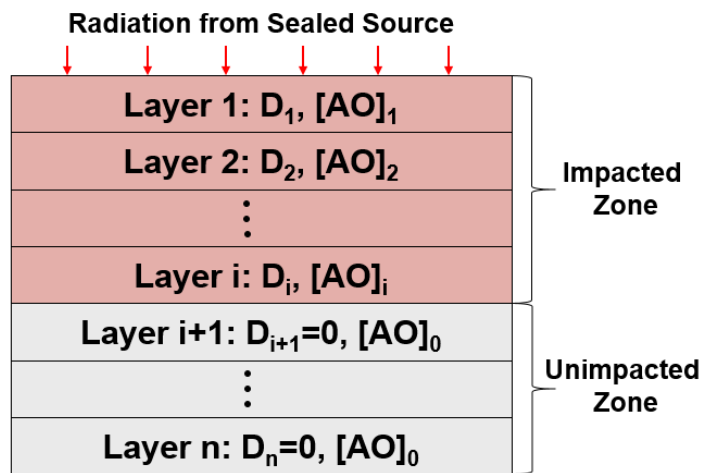


Fig. 4. Layering in multilayer model for antioxidant depletion in HDPE GM exposed to radiation with antioxidant concentration $[AO]_i$ after exposure to radiation dosage D_i . Each layer in un-impacted zone (no dose) has the initial antioxidant concentration $[AO]_0$.

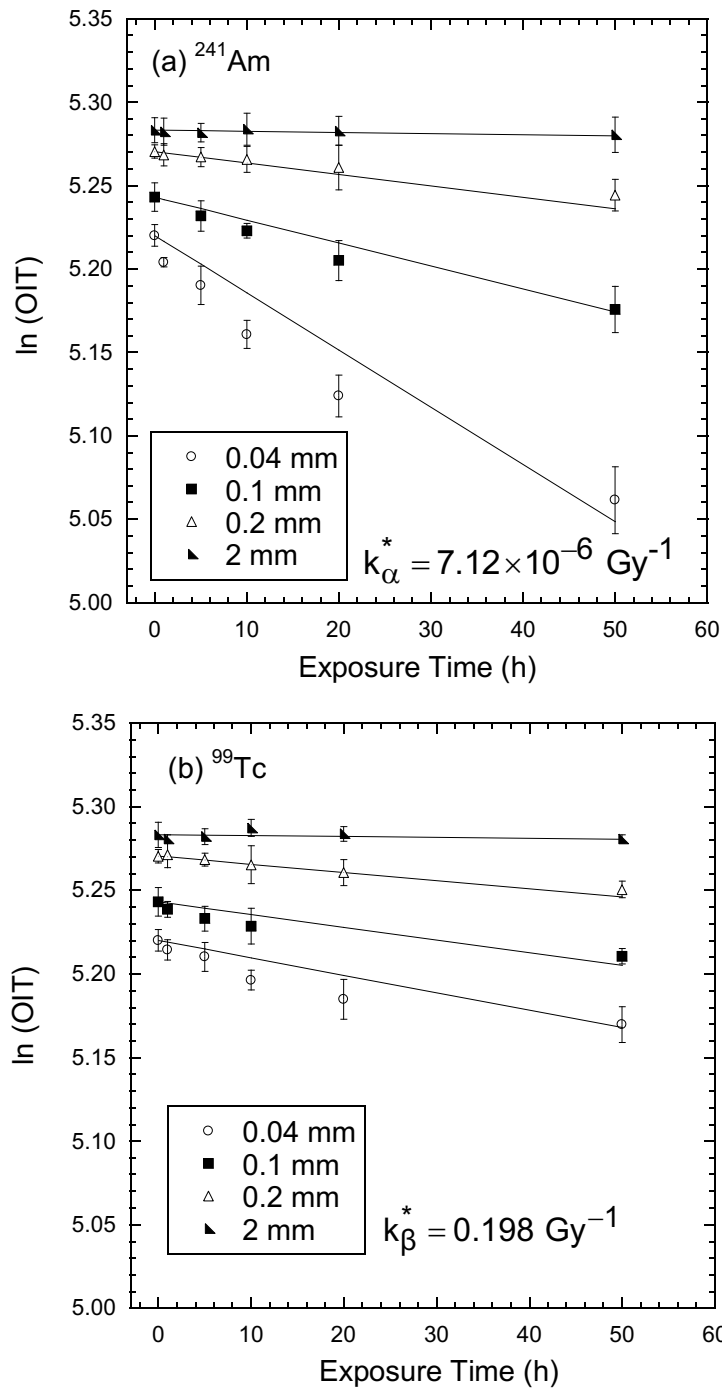


Fig. 5. Fit of Eq. 10 to obtain k^* using OIT data for 0.04, 0.1, 0.2, and 2-mm-thick HDPE GM specimens after exposure to sealed sources of ^{241}Am (a) and ^{99}Tc (b) for up to 50 h. Fit made using simultaneous regression on data from all specimens.

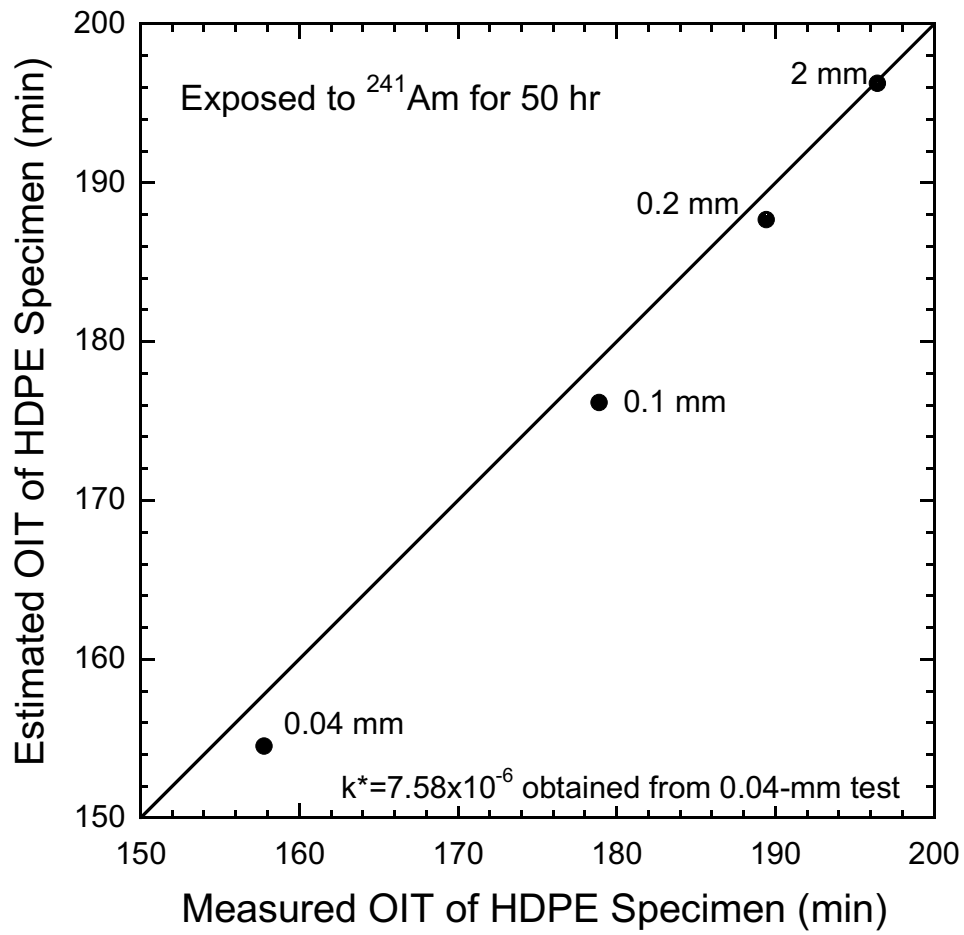


Fig. 6. Measured OIT vs. Estimated OIT of HDPE specimens exposed to sealed source of ^{241}Am for 50 hr [units for k^* in $\ln(\text{min})/\text{Gy}$].

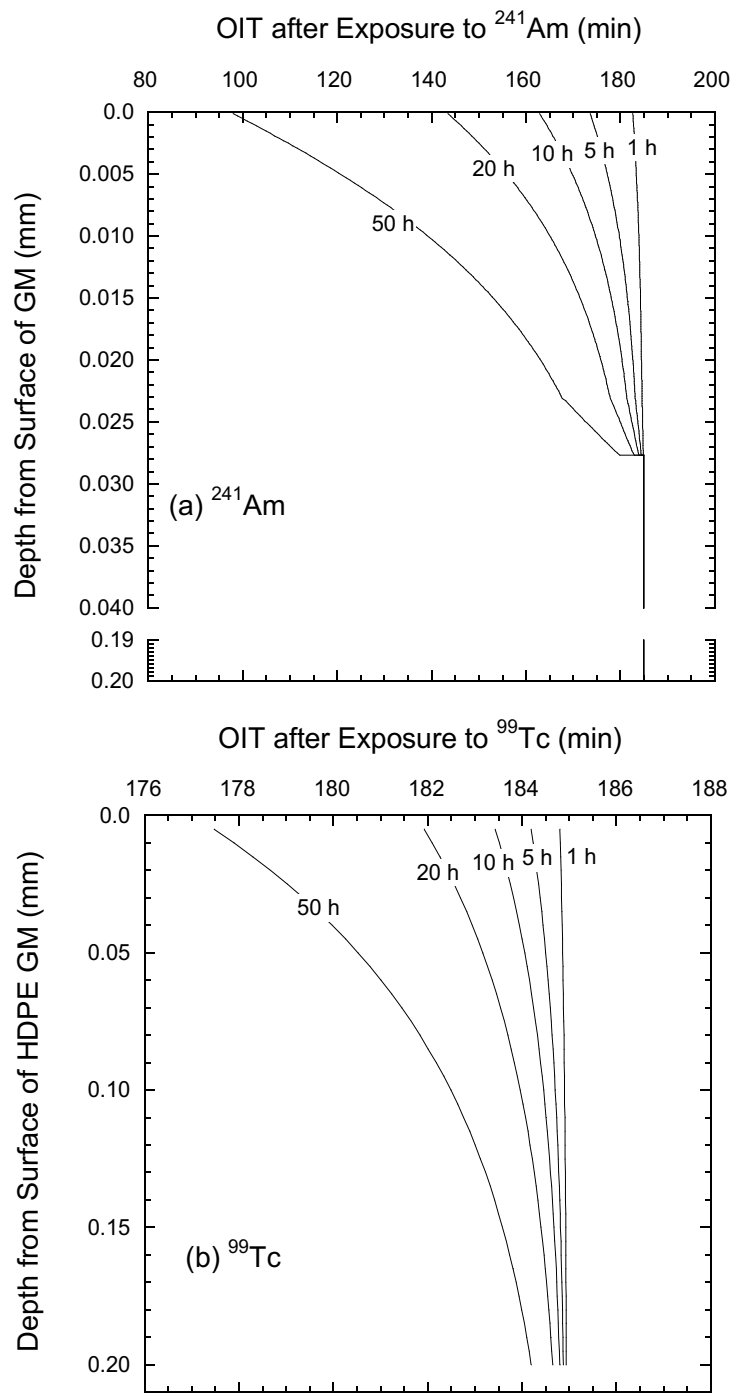


Fig. 7. OIT as a function of depth from surface of GM computed using multilayer model for 0.2-mm-thick HDPE GM exposed to sealed source of ^{241}Am (a) or sealed source of ^{99}Tc (b).

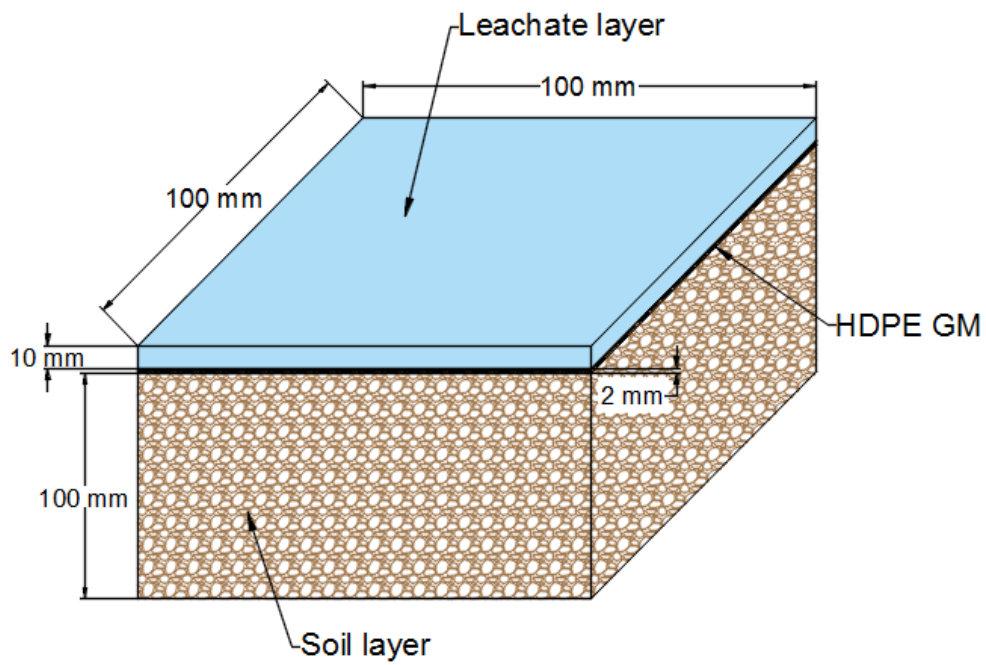


Fig. 8. Domain simulated with GEANT4 representing composite liner with HDPE GM on compacted clay liner with thin layer of LLE leachate pooled above. LLW leachate assumed to contain radionuclides and major cations and anions in Table 2 based on the leachate characterization reported in Tian et al. (2016, 2017a).

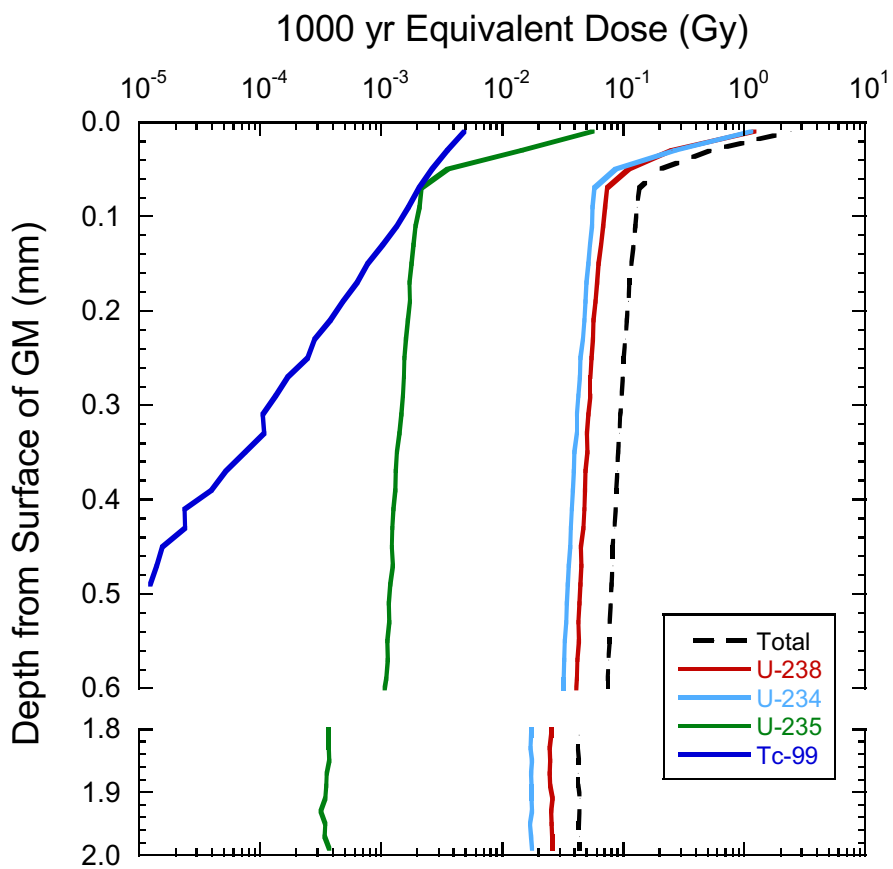


Fig. 9. Dose as function of depth in HDPE GM in a composite liner overlain with LLW leachate after 1000 yr of exposure as predicted with GEANT4.

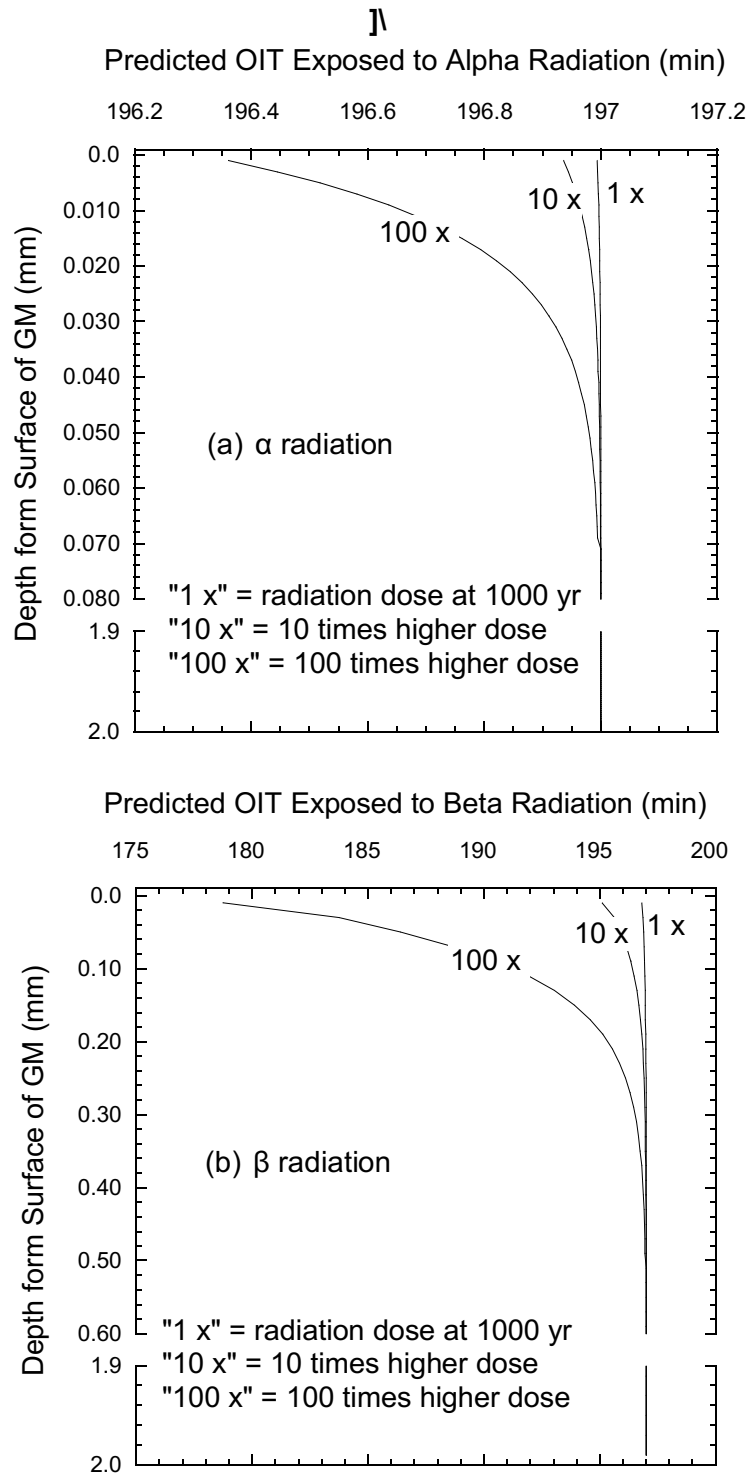


Fig. 10. OIT as a function of depth in HDPE GM exposed to α (a) and β (b) radiation for 1000 yr for base case and doses 10x and 100x higher than dose for base case.

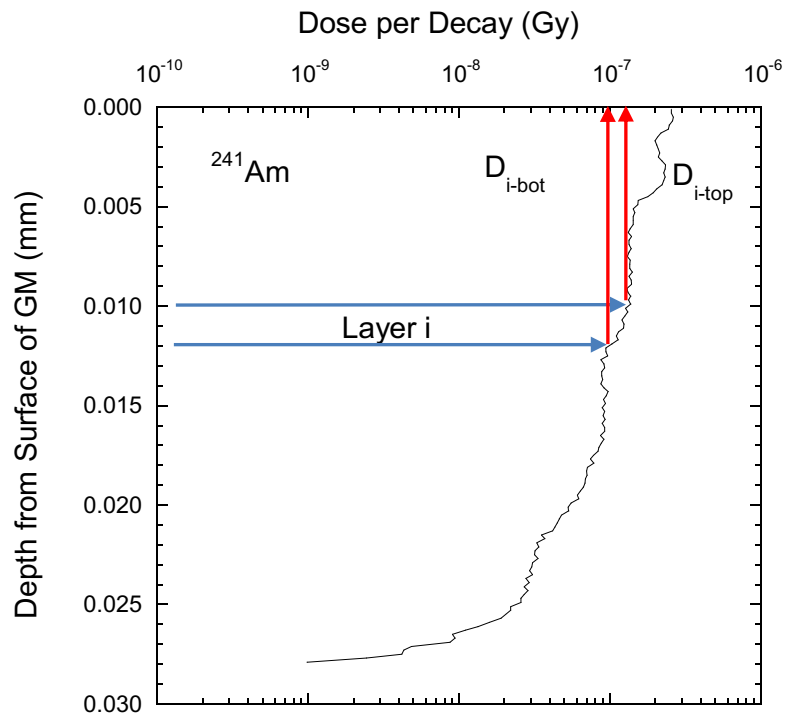


Fig. A1. Dose per decay as a function of depth from the surface of the GM predicted by GEANT4 for HDPE GM exposed to a sealed source of ^{241}Am .

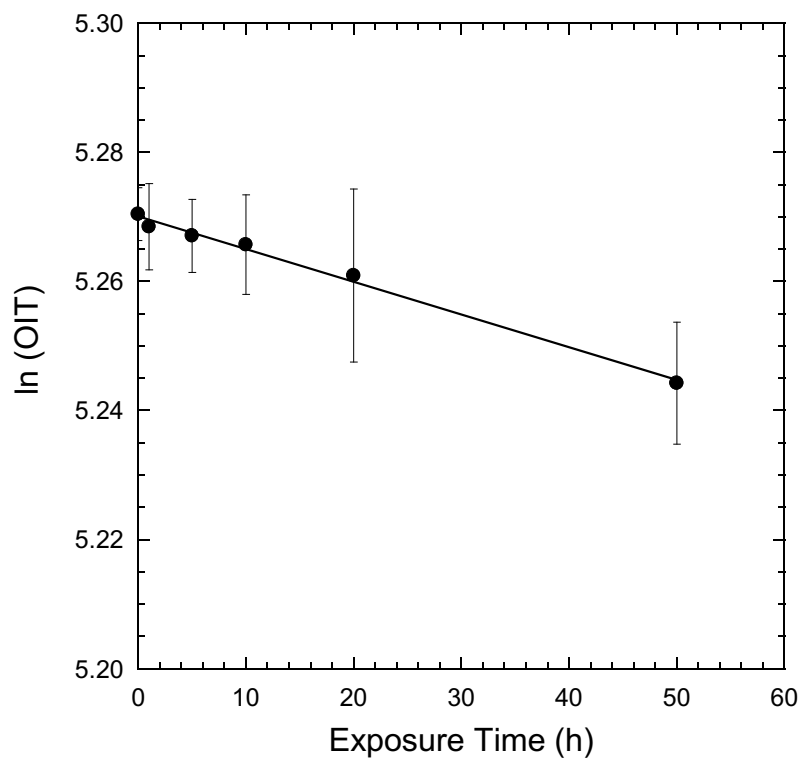


Fig. A2. Fit of multilayer model Eq. A3 (solid line) to OIT data for 0.2-mm-thick HDPE GM specimens after exposure to sealed sources of ^{241}Am for up to 50 h.